

Mean moment effect on circular thin-walled tubes under cyclic bending

Kao-Hua Chang[†] and Wen-Fung Pan[‡]

Department of Engineering Science, National Cheng Kung University, Tainan, Taiwan 701, R.O.C.

Kuo-Long Lee^{‡†}

Department of Computer Application Engineering, Far East College, Tainan County, Taiwan 744, R.O.C.

(Received September 27, 2005, Accepted November 22, 2007)

Abstract. In this paper, experimental and theoretical investigations of the effect of the mean moment on the response and collapse of circular thin-walled tubes subjected to cyclic bending are discussed. To highlight the influence of the mean moment effect, three different moment ratios r (minimum moment/maximum moment) of -1 , -0.5 and 0 , respectively, were experimentally investigated. It has been found that the moment-curvature loop gradually shrinks with the number of cycles, and becomes stable after a few cycles for symmetric cyclic bending ($r = -1$). However, the moment-curvature loop exhibits ratcheting and increases with the number of cycles for unsymmetric cyclic bending ($r = -0.5$ or 0). In addition, although the three groups of tested specimens had three different moment ratios, when plotted in a log-log scale, three parallel straight lines describe the relationship between the controlled moment range and the number of cycles necessary to produce buckling. Finally, the endochronic theory combined with the principle of virtual work was used to simulate the relationship among the moment, curvature and ovalization of thin-walled tubes under cyclic bending. An empirical formulation was proposed for simulating the relationship between the moment range and the number of cycles necessary to produce buckling for thin-walled tubes subjected to cyclic bending with different moment ratios. The results of the experimental investigation and the simulation are in good agreement with each other.

Keywords: moment-controlled; mean moment; moment ratio; thin-walled tube; cyclic bending; ovalization; collapse; endochronic theory.

1. Introduction

In practice, many industrial thin-walled tube components or structures, such as the structures of buildings in earthquake-prone areas, offshore pipelines, heat exchangers in power plants and nuclear reactors, etc., are constantly subjected to cyclic bending. The bending of thin-walled tubes leads to the ovalization of the tube cross section. Reverse bending and subsequent repeated cyclic bending will cause a gradual growth of the ovalization. The increasing ovalization causes a progressive

[†] Graduate Student, E-mail: kfchuang@cc.kuas.edu.tw

[‡] Professor, Corresponding author, E-mail: pan@phoebus.es.ncku.edu.tw

^{‡†} Associate Professor, E-mail: lkl@cc.fec.edu.tw

reduction in the bending rigidity of the tube. The tube will buckle when a critical magnitude of ovalization is reached. It is therefore of great importance to understand the response and collapse of thin-walled tubes under cyclic bending in many industrial applications.

The tube bending has been experimentally and theoretically investigated under monotonic bending with or without external pressure. Fabian (1977) studied the nonlinear pre-buckling state and the bifurcation and initial post-buckling behavior of infinitely long cylindrical elastic tubes under bending, external pressure and axial loads. Reddy (1979) conducted a series of tests on aluminum alloy and steel tubes, which buckle in the plastic range under pure bending and uniform axial compression. Gellin (1980) investigated the effects of nonlinear material buckling behavior for an infinitely long cylindrical shell under pure bending. Kyriakides and Shaw (1982) investigated the response and stability of elastoplastic pipes under monotonic bending and external pressure.

Kyriakides and his co-workers designed and constructed the tube cyclic bending machine as shown in Fig. 1(a), and conducted a series of experimental and theoretical investigations. Shaw and Kyriakides (1985) investigated the inelastic behavior of 6061-T6 aluminum and 1018 steel tubes subjected to cyclic bending. Kyriakides and Shaw (1987) extended the analysis of 6061-T6 aluminum and 1018 steel tubes to the stability conditions under cyclic bending. Corona and Kyriakides (1988) investigated the stability of 304 stainless steel tubes subjected to combined bending and external pressure. Corona and Kyriakides (1991) studied the degradation and buckling of 6061-T6 aluminum and 1020 carbon steel tubes under cyclic bending and external pressure. Corona and Vaze (1996) studied the response, buckling and collapse of long, thin-walled seamless steel square tubes under bending. Vaze and Corona (1998) experimentally investigated the elastic-plastic degradation and collapse of steel tubes with square cross-sections under cyclic bending.

Pan and his co-workers also constructed a similar bending machine with a newly invented measurement apparatus, which was designed and set up by Pan *et al.* (1998), to study various kinds of tubes under different cyclic bending conditions. Pan and Fan (1998) studied the effect of the prior curvature-rate at the preloading stage on the subsequent creep (hold constant moment for a period of time) or relaxation (hold constant curvature for a period of time) behavior. Pan and Her (1998) investigated the response and stability of SUS 304 stainless steel tubes subjected to cyclic bending with different curvature-rates. Lee *et al.* (2001) studied the influence of the diameter-to-thickness ratio (D/t ratio) on the response and stability of circular tubes subjected to symmetrical cyclic bending. Lee *et al.* (2004) investigated experimentally the effect of the D/t ratio and curvature-rate on the response and stability of circular tubes subjected to cyclic bending.

In addition, Elchalakani *et al.* (2002) experimentally conducted tests on the different D/t ratios of grade C350 steel tubes under pure bending, and proposed two theoretical simulation models. Jiao and Zhao (2004) tested the bending behavior of very high strength (VHS) circular steel tubes, and proposed their plastic slenderness limit. Elchalakani *et al.* (2004) experimentally investigated the inelastic flexural behavior of concrete-filled tubular (CFT) beams, which were made of cold-formed circular hollow sections and filled with normal concrete.

As for circular tubes subjected to unsymmetric bending, Corona and Kyriakides (1991) were the first to experimentally investigate the response of circular tubes under curvature-controlled cyclic bending with a non-zero mean curvature (mean value = (maximum curvature + minimum curvature)/2). The experimental moment-curvature loop shows that the 1020 carbon steel tube relaxes cyclically for the first few cycles. However, after a few cycles, the loop gradually stabilizes. The ovalization-curvature curve indicates that the ovalization increases in a ratcheting manner with the number of cycles. In addition, the ovalization-curvature curve is biased in the direction of the mean

curvature. The rate at which ovalization accumulates was found not to be significantly affected by the mean curvature in the cycles. Thereafter, Pan and Lee (2002) systematically studied the response of thin-walled tubes under curvature-controlled cyclic bending with an averaged curvature. They used the first-order ordinary differential constitutive equations of the endochronic theory to simulate the response of the thin-walled tubes subjected to cyclic bending with an averaged curvature. Furthermore, they proposed a theoretical formulation to simulate the relationship between the curvature range and the number of cycles which produces buckling for different curvature ratios (minimum curvature/maximum curvature). They achieved good agreement between the experimental and theoretical results.

Another aspect of unsymmetric bending, namely moment-controlled bending, has not been investigated experimentally and theoretically yet. The response and collapse for moment-controlled loading are more complicated than for curvature-controlled bending. Since no research regarding this aspect could be found in the literature, a systematic study on the response and collapse of thin-walled tubes subjected to cyclic bending with different mean moments was proposed. A four-point bending machine and a curvature-ovalization measurement apparatus, designed and reported previously by Pan *et al.* (1998), were used to conduct a series of moment-controlled cyclic bending tests. The material of thin-walled tubes used for this study was SUS 304 stainless steel tubes. The magnitude of the bending moment was measured using two load cells, mounted in the bending device, and the magnitudes of the curvature and the ovalization of the tube cross-section were measured using the curvature-ovalization measurement apparatus. The number of cycles necessary to produce buckling was also recorded during the test. To highlight the influence of the mean moment effect, three different moment ratios r , -1 , -0.5 and 0 , were experimentally investigated in this study. The endochronic theory combined with the principle of virtual work was used to simulate the response of thin-walled tubes under unsymmetric cyclic bending. The response is dependant on the bending moment, tube curvature and ovalization of the tube cross-section. An empirical formula was proposed which can be used to simulate the relationship between the controlled-moment range and the number of cycles that producing buckling with different moment ratios. The theoretical simulation is in good agreement with the obtained experimental results.

2. Experimental facility, specimens and test procedures

In this study, the cyclic pure bending experiments on thin-walled tubes were conducted using a pure bending device and a curvature-ovalization measurement apparatus (COMA) located in the Department of Engineering Science at the National Cheng Kung University.

2.1 Bending device

A schematic drawing and a picture of the bending device are shown in Figs. 1(a) and 1(b), respectively. It is designed as a four-point bending machine, capable of applying reverse cyclic bending. The device consists of two rotating sprockets resting on two support beams. Heavy chains run around the sprockets, which rest on two heavy support beams 1.25 m apart. This allows the maximum length of the test specimen to be 1 m. The bending capacity of the machine is 5300 N-m. Each tube is tested and fitted with a solid rod extension. The contact between the tube and the rollers is free to move along the axial direction during bending. The load transfer to the test

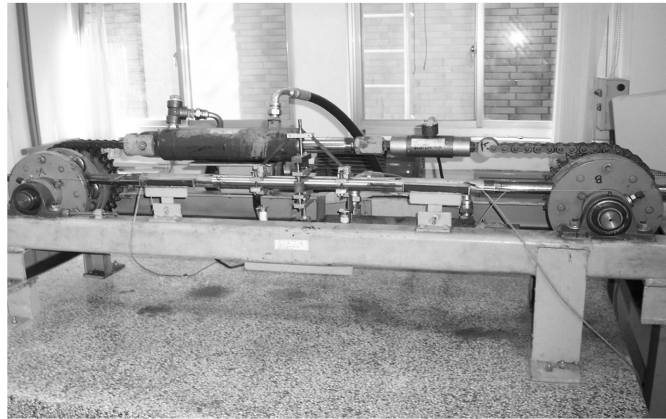
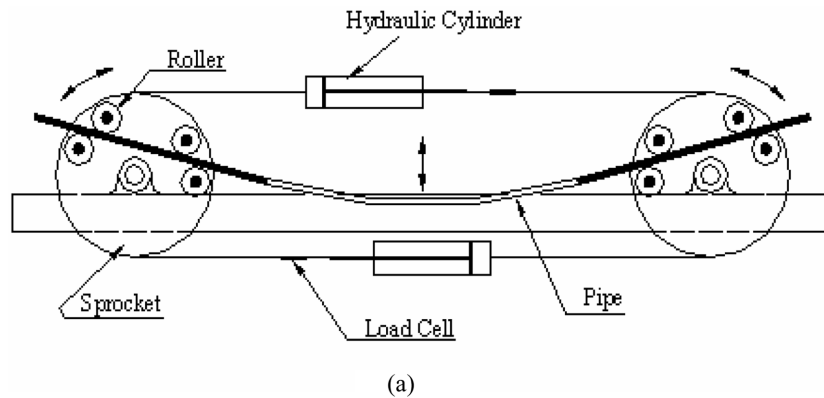


Fig. 1 The bending device of (a) a schematic drawing and (b) a picture

specimen is formed by concentrated loads from two of rollers in the form of a couple. Once either the top or bottom cylinder is contracted, the sprockets are rotated, and pure bending of the test specimen is achieved. Reverse bending can be achieved by reversing the flow direction in the hydraulic circuit.

2.2 Curvature-ovalization measurement apparatus (COMA)

COMA is an instrument used to measure the tube curvature and ovalization of a tube cross-section. Figs. 2(a) and 2(b) show a schematic drawing and a picture of the COMA. It is a lightweight instrument, which can be mounted close to the tube mid-span. There are three inclinometers in the COMA. Two inclinometers are fixed on two holders, which are denoted as side-inclinometers (see Fig. 2(b)). These holders are fixed on the circular tube before the test begins. Based on the fixed distance between the two side-inclinometers and the angle changes detected by the two side-inclinometers, the tube curvature can be obtained by simple calculation. In addition, by using the magnetic detector on the middle part of COMA to measure the change of the outside diameter, the ovalization of the tube cross-section can be determined. Detailed descriptions of the bending device and the COMA has been detailed by Pan *et al.* (1998).

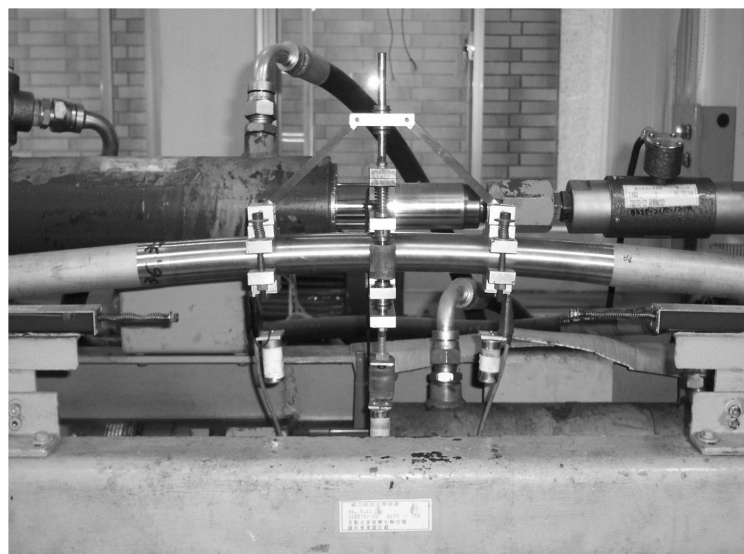
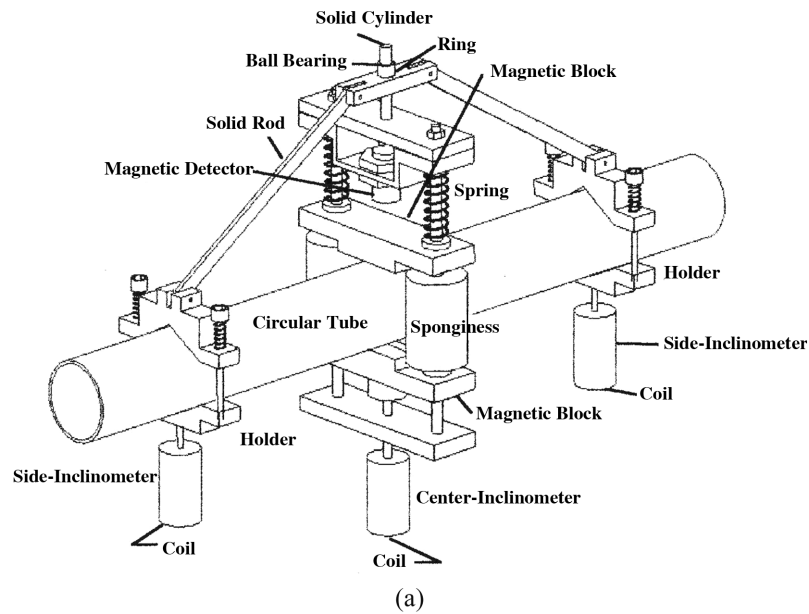


Fig. 2 The COMA of (a) a schematic drawing and (b) a picture

2.3 Material and specimens

The material used in this study was thin-walled tubes made of SUS 304 stainless steel. The tube's chemical composition (in mass percentages) is Cr 18.36, Ni 8.43, Mn 1.81, Si 0.39, C 0.005, P 0.28, S 0.04, and the remainder Fe. The SUS 304 stainless steel's yield stress was 205 MPa, and its ultimate tensile stress was 520 MPa with a 35% percent elongation. The D/t ratio was selected to be 60 in this study. The tested specimens initially had a nominal outside diameter D of 38.1 mm and a

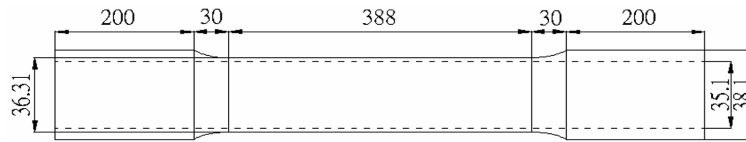


Fig. 3 Dimensions of the tested specimens

wall thickness t of 1.5 mm ($D/t = 25.4$). In order to obtain the desired D/t ratio, the outside diameter of the raw specimens $D = 38.1$ mm had to be machined to obtain an outside diameter of 36.31 mm. However, the inside diameter was left intact and had the same magnitude for all tested specimens (inside diameter = 35.1 mm). Fig. 3 shows the dimensions of the test specimens.

3. Theoretical formulation

In this section, the elastoplastic response of the SUS 304 stainless steel tubes subjected to cyclic bending is analyzed. The kinematics of the tube cross section, the constitutive model and the principle of virtual work are discussed separately.

3.1 Kinematics

A circular tube subjected to cyclic bending is considered in this study. Fig. 4 shows the problem geometry, in which R_m is the mean radius, and t is the wall thickness. Based on the axial, circumferential, and radial coordinates x , θ and r , the displacements of a point on the tube's mid-surface are denoted as u , v and w , respectively.

The kinematic relations required must be general enough to accommodate ovalization of the cross-section. Such a set of relations has been developed by Gellin (1980) and used successfully by Kyriakides and Shaw (1982). Briefly, it is assumed that the plane sections perpendicular to the tube mid-surfaces before and during deformation. The strains are assumed to remain small but finite rotations about both axes of bending are allowed. The axial strain is expressed as (Kyriakides and Shaw 1982, Shaw and Kyriakides 1985, Kyriakides and Shaw 1987)

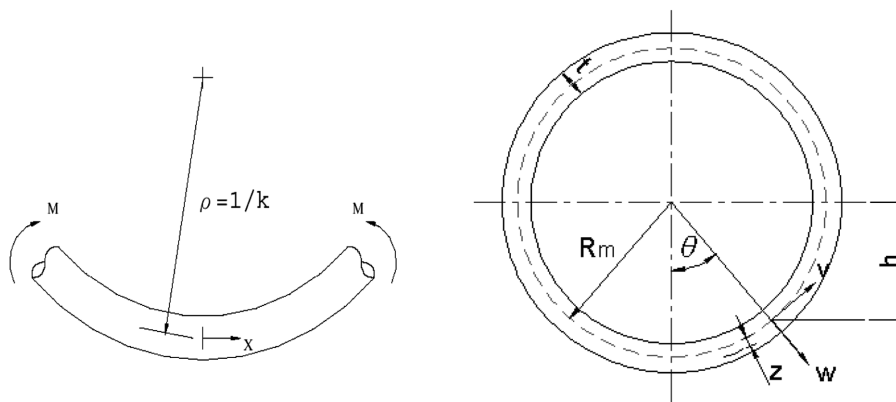


Fig. 4 Problem geometry of circular tube subjected to pure bending

$$\varepsilon_x = \varepsilon_x^0 + h \cdot \kappa \tag{1}$$

and

$$h = (R_m + w)\cos \theta - v\sin \theta + Z\cos \theta \tag{2}$$

where ε_x^0 is the axial strain of the cylinder's axis, h is distance between the point and the horizontal plane passing through the center of the cross-section, κ is the tube curvature and Z is the distance between the point and the midpoint surface. The circumferential strain is

$$\varepsilon_\theta = \varepsilon_\theta^0 + h \kappa_\theta \tag{3}$$

where

$$\varepsilon_\theta^0 = \frac{(v' + w)}{R_m} + \frac{1}{2} \left(\frac{v' + w}{R_m} \right)^2 + \frac{1}{2} \left(\frac{v - w'}{R_m} \right)^2 \tag{4}$$

and

$$\kappa_\theta = \left(\frac{v' - w''}{R_m^2} \right) / \sqrt{1 - \left(\frac{v - w'}{R_m} \right)^2} \tag{5}$$

(\cdot) denotes the differentiation with respect to θ .

3.2 Endochronic constitutive equations

Based on the assumption of small deformation for homogeneous and isotropic materials, the increment of the deviatoric stress tensor $d\underline{s}$ of the endochronic theory is given as (Valanis 1980)

$$d\underline{s} = 2\rho(0)d\underline{e}^p + 2\underline{h}(z)dz \tag{6}$$

and

$$\underline{h}(z) = \int_0^z \frac{d\rho(z-z')}{dz} \frac{\partial \underline{e}^p}{\partial z'} \tag{7}$$

where z is the intrinsic time scale, $\rho(z)$ is termed the kernel function, and \underline{e}^p is the deviatoric plastic strain tensor which is defined as

$$d\underline{e}^p = d\underline{e} - \frac{d\underline{s}}{2\mu_0} \tag{8}$$

where \underline{e} denotes the deviatoric strain tensor, and μ_0 is the elastic shear modulus. The intrinsic time measure ζ is

$$d\zeta = \|d\underline{e}^p\| \tag{9}$$

in which $\| \cdot \|$ represents the Euclidean norm. The intrinsic time scale z is

$$dz = \frac{d\zeta}{f(\zeta)} \tag{10}$$

where $f(\zeta)$ is a material hardening function which can be expressed as

$$f(\zeta) = 1 - Ce^{-\beta\zeta}, \quad \text{for } C < 1 \quad (11)$$

in which C and β are material parameters. If plastic incompressibility is satisfied, the elastic hydrostatic response can be written as

$$d\sigma_{kk} = 3Kd\varepsilon_{kk} \quad (12)$$

where σ_{kk} and ε_{kk} are the traces of stress and strain tensors, respectively, and K is the elastic bulk modulus. According to the mathematical characteristic of the kernel function $\rho(z)$, Eq. (6) is expressed as (Pan *et al.* 1996, Pan and Chern 1997)

$$d\zeta = \sum_{i=1}^n ds_i = 2 \sum_{i=1}^n C_i d\zeta^p - \sum_{i=1}^n \alpha_i \zeta_i dz \quad (13)$$

Where C_i and α_i are material constants. Substituting Eq. (8) into Eq. (13) leads to

$$d\zeta = \frac{\mu_0}{\mu_0 + \sum_{i=1}^n C_i} \left[2 \sum_{i=1}^n C_i d\zeta^p - \sum_{i=1}^n \alpha_i \zeta_i dz \right] \quad (14)$$

By using Eq. (12), Eq. (14) can be expressed in terms of the stress and strain tensors as

$$d\zeta = p_1 d\varepsilon + p_2 d\varepsilon_{kk} I + p_3 \sum_{i=1}^n \alpha_i \left(\zeta - \frac{\sigma_{kk}}{3} I \right)_i dz \quad (15)$$

where

$$p_1 = \frac{2\rho(0)}{1 + \frac{\rho(0)}{\mu_0}}, \quad p_0 = K - \frac{2\rho(0)}{3\left(1 + \frac{\rho(0)}{\mu_0}\right)}, \quad p_2 = \frac{1}{1 + \frac{\rho(0)}{\mu_0}} \quad (16)$$

3.3 Principle of virtual work

The principle of virtual work, which satisfies the equilibrium requirement, is given by

$$\int_V \sigma_{ij} \delta \varepsilon_{ij} dV = \delta W \quad (17)$$

where V is the volume of the material of the tube section considered, and δW is the virtual work of the external loads. For the case of a circular tube subjected to cyclic bending, the quantity of δW for the incremental loading can be expressed as

$$\int_V (\sigma_{ij} + \dot{\sigma}_{ij}) \delta \varepsilon_{ij} dV = 2R \int_{0-t/2}^{\pi/2} \int [\dot{\sigma}_x \delta \varepsilon_x] dT d\theta = 0 \quad (18)$$

where $\dot{\sigma}_x = \sigma + \sigma_x$ and $(\dot{\quad})$ denotes the increment of (\quad) . The in-plane displacements v and w are

assumed to be symmetrical and are approximated by the following expression (Shaw and Kyriakides 1985, Kyriakides and Shaw 1987)

$$v \cong R_m \sum_{n=2}^N a_n \sin n \theta, \quad w \cong R_m \sum_{n=0}^N b_n \cos n \theta \quad (19)$$

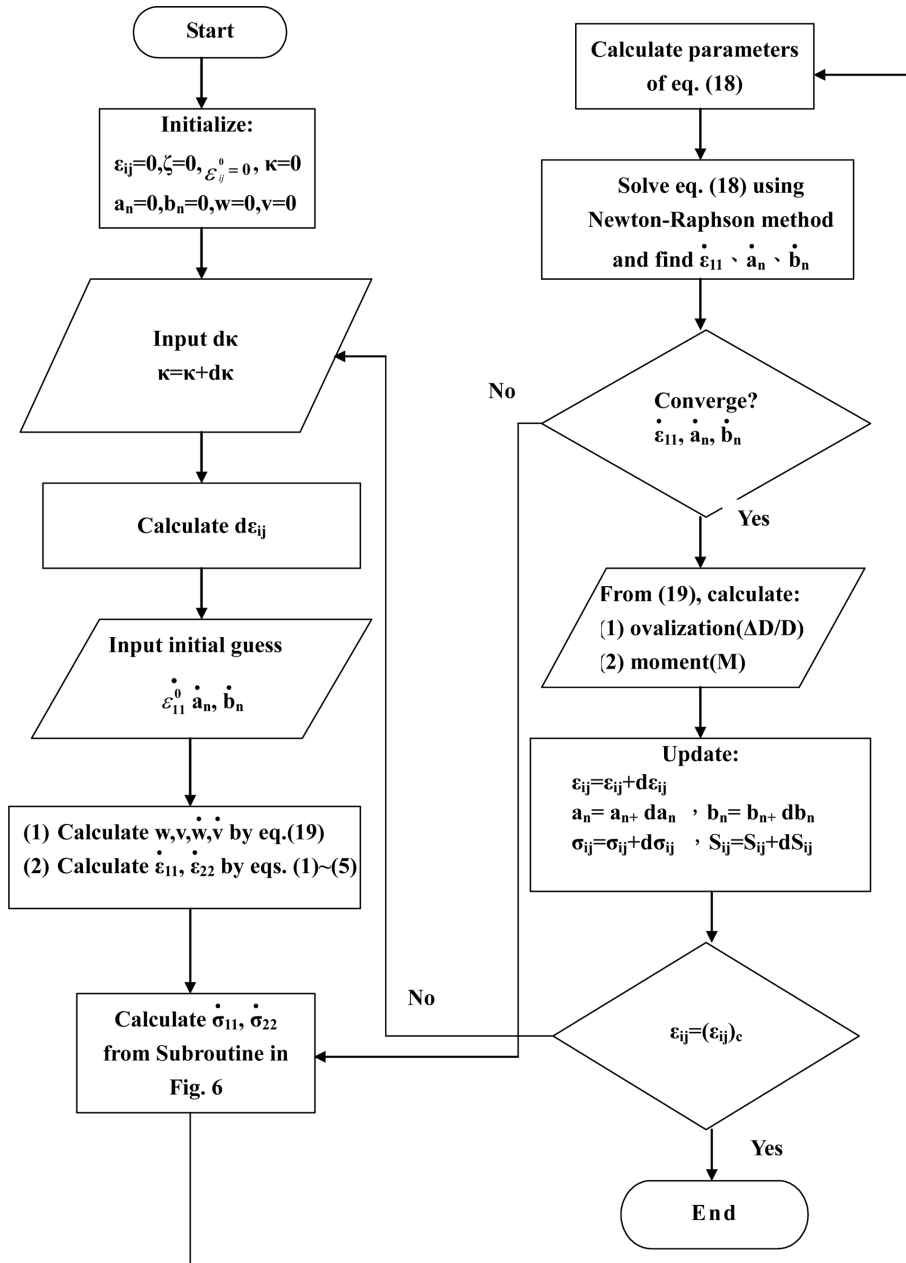


Fig. 5 Flow chart of numerical solution procedure

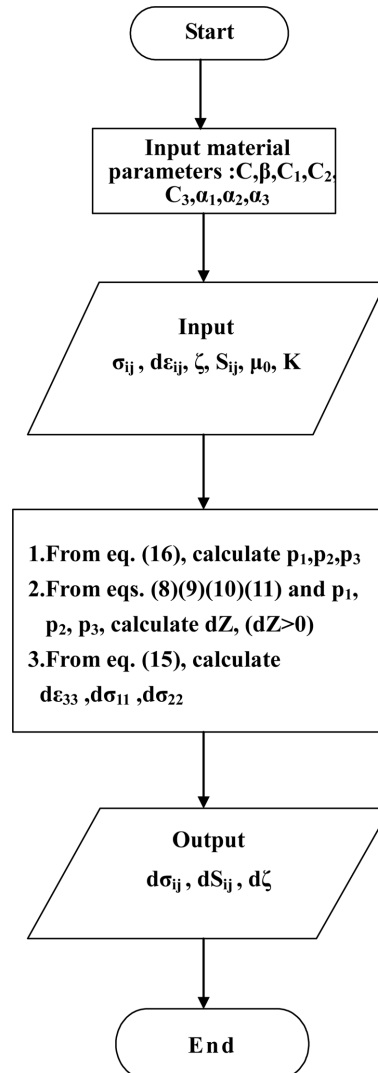


Fig. 6 Flow chart of the calculation of the endochronic theory

where the number of terms N is chosen to ensure satisfactory convergence. Kyriakides and Shaw (1987) investigated the sensitivity of the moment-curvature and ovalization- curvature response for monotonic pure bending to the number of expansion terms used in Eq. (19). Those equations clearly indicate that $N = 4$ or 6 is sufficient. By substituting Eqs. (1)-(5), (19) into Eq. (18), a system of $2N + 1$ nonlinear algebraic equations in terms of $\dot{a}_2, \dot{a}_3, \dots, \dot{b}_0, \dot{b}_1, \dot{b}_2, \dots, \epsilon_x^0$ are determined. This system of equations is solved using the Newton-Raphson method. The iterative scheme contains nested iterations for the constitutive relations. Kyriakides and Shaw (1987) provide a more detailed derivation of the equation system. Fig. 5 shows the main steps of the numerical solution in a flow chart. In addition, the steps of calculating the stress-strain relationship using endochronic theory is demonstrated in a flow chart in Fig. 6

4. Results and discussions

In this section, we show the theoretical and experimental results of the response and collapse for SUS 304 stainless steel tubes subjected to symmetric and unsymmetric moment-controlled cyclic bending. In the theoretical study, the kernel function of the endochronic theory was considered to be composed of three terms of exponentially decaying functions. Because of this fact, the material parameters of the theory can be determined according to the method proposed by Fan (1983). The material parameters were determined to be: $\mu_0 = 70$ GPa, $K = 150$ GPa, $C_1 = 5.2 \times 10^6$ MPa, $\alpha_1 = 2560$, $C_2 = 6.0 \times 10^5$ MPa, $\alpha_2 = 1050$, $C_3 = 4.0 \times 10^4$ MPa, $\alpha_3 = 200$, $C = 0.63$ and $\beta = 1.5$. In addition, based on the experimental results, an empirical formulation for the relationship between the moment range and the number of cycles necessary to produce buckling is proposed. Furthermore, an empirical formulation for the relationship between the critical magnitude of ovalization at collapse and the controlled moment range is also introduced.

4.1 Response of SUS 304 stainless steel tubes under moment-controlled symmetric and unsymmetric cyclic bending

Fig. 7(a) shows the experimentally determined cyclic moment (M)-curvature (κ) curve for moment-controlled symmetric cyclic bending with a controlled moment range from +150 to -150 N-m. The moment ratio r is -1. It can be seen that the first M - κ loop is on the left side, but the subsequent M - κ loops gradually move toward the right with an increasing number of cycles. Finally, the M - κ loop becomes steady after a few cycles. Fig. 7(b) depicts the corresponding theoretical (simulated) results.

Fig. 8(a) shows the corresponding experimental results for the cyclic ovalization ($\Delta D/D$) - moment (M) curve. The ovalization is seen to be continuously changing. On first loading, the

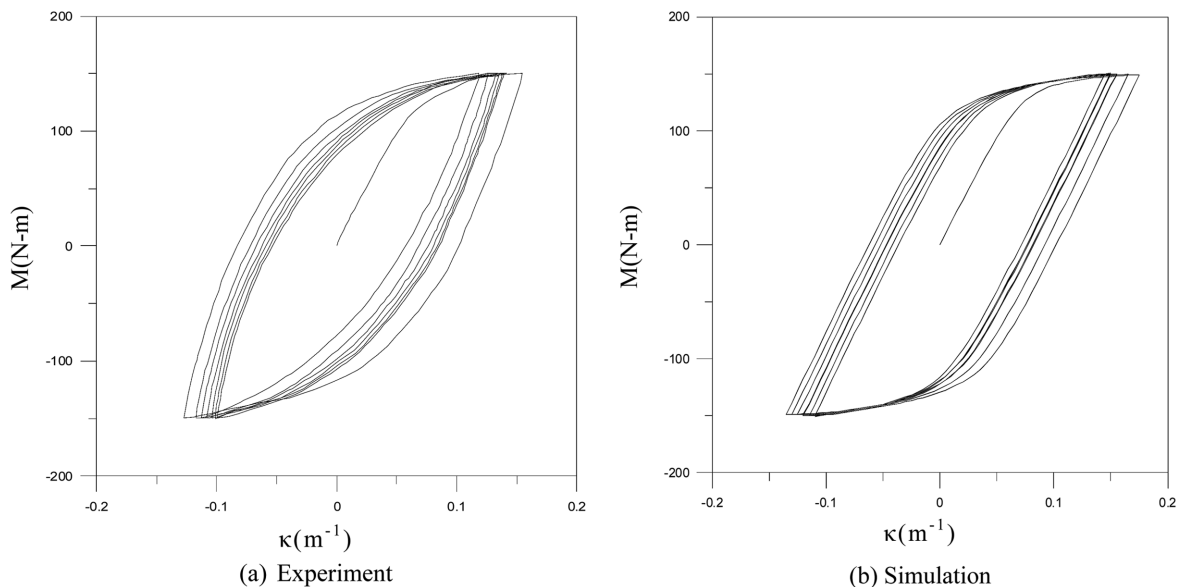


Fig. 7 Experimental and simulated cyclic moment (M)-curvature (κ) curve where the moment ranges from +150 to -150 N-m ($r = -1$)

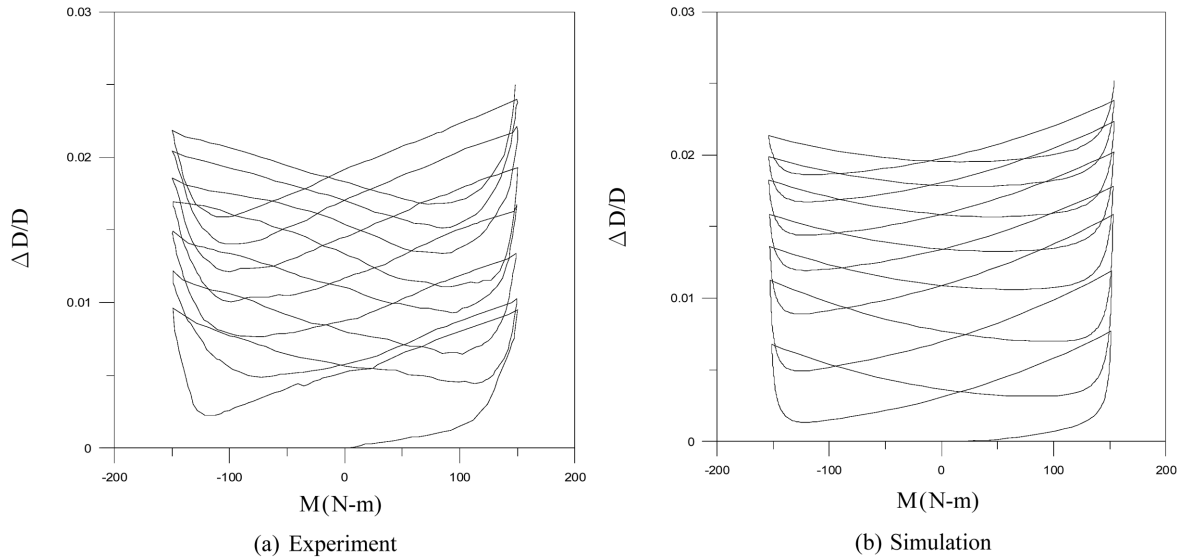


Fig. 8 Experimental and simulated cyclic ovalization ($\Delta D/D$)-moment (M) curve where the moment ranges from +150 to -150 N-m ($r = -1$)

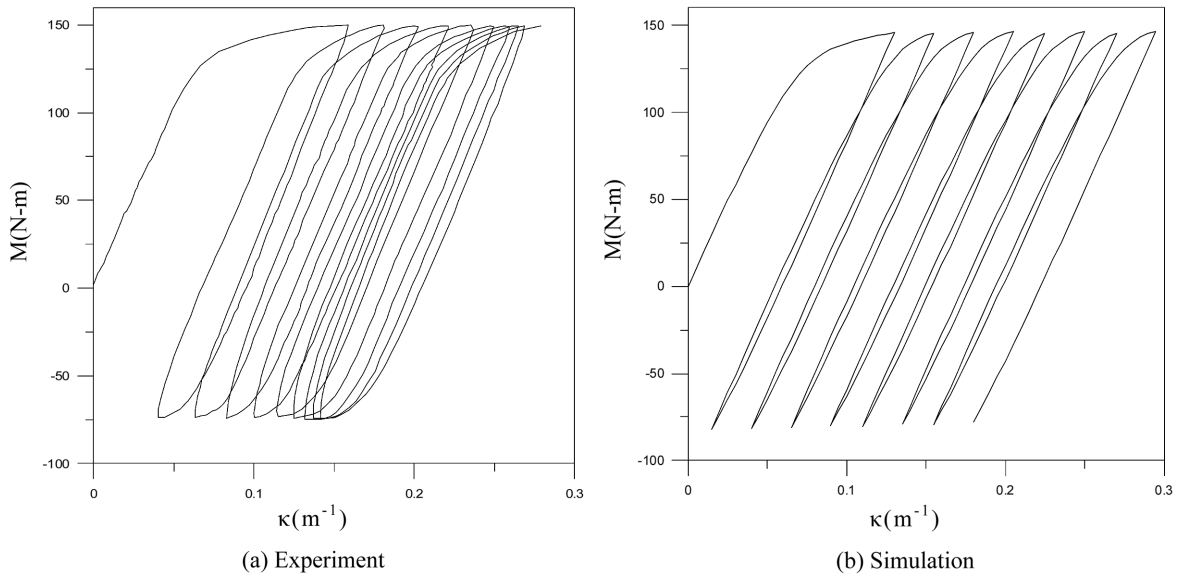


Fig. 9 Experimental and simulated cyclic moment (M)-curvature (κ) curve where the moment ranges from +150 to -75 N-m ($r = -0.5$)

ovalization grows to a maximum value at the controlled maximum moment. On unloading to zero moment, some permanent deformation of the tube cross section is observed. Continuous reverse bending to the minimum moment causes the ovalization to increase again. The ovalization increases in a symmetric and ratcheting manner with the number of bending cycles. The ovalization continues to progress until a certain critical value is achieved at which the tube buckles. Fig. 8(b) depicts the corresponding theoretical results.

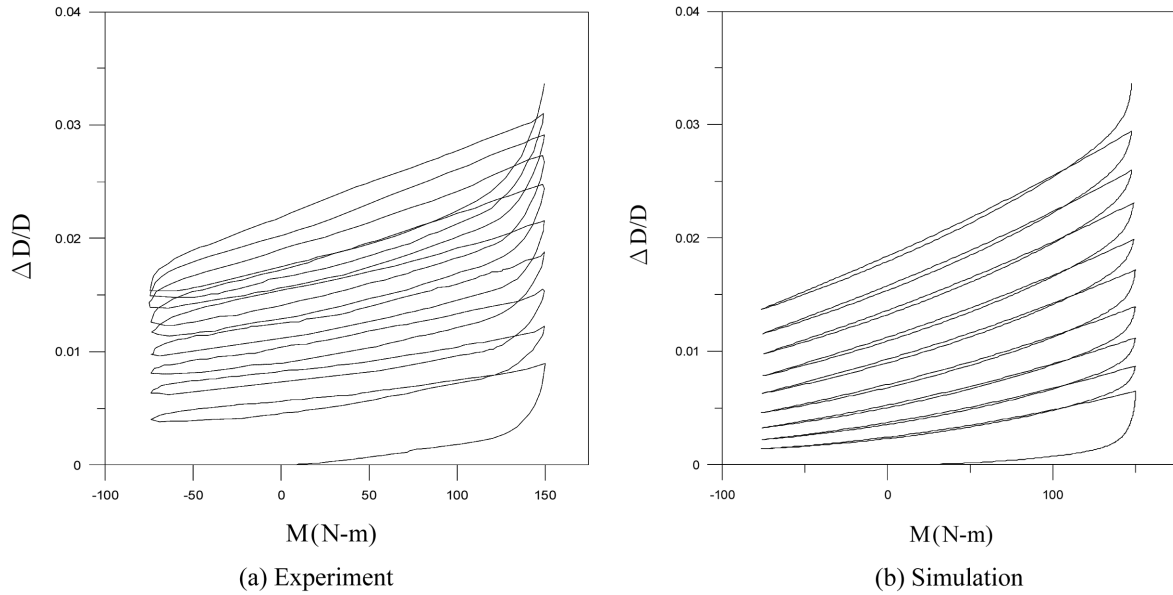


Fig. 10 Experimental and simulated cyclic ovalization ($\Delta D/D$)-moment (M) curve where the moment ranges from + 150 to -75 N-m ($r = -0.5$)

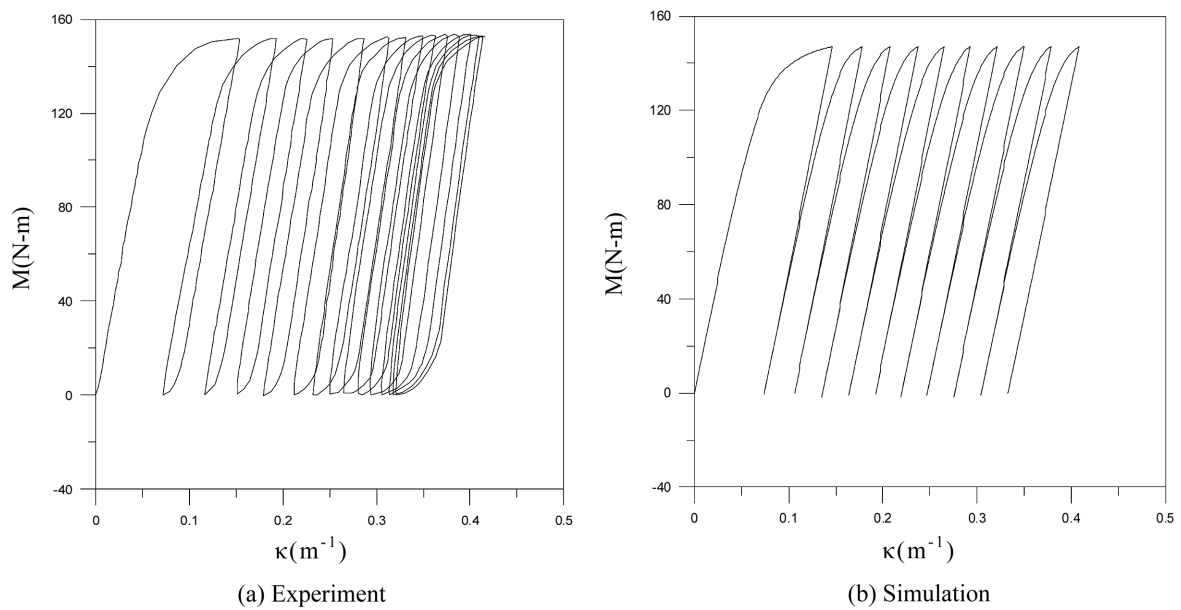


Fig. 11 Experimental and simulated cyclic moment (M)-curvature (κ) curve where the moment ranges from + 150 to 0 N-m ($r = 0$)

Figs. 9(a) and 11(a) show the experimental cyclic M - κ curve for the controlled moment ranges from + 150 to -75 N-m and + 150 to 0 N-m, respectively. These two cases demonstrate moment-controlled unsymmetric cyclic bending with the values of $r = -0.5$ and 0, respectively. It can be seen that the M - κ curve ratchets to the right with an increasing number of cycles. The ratcheting

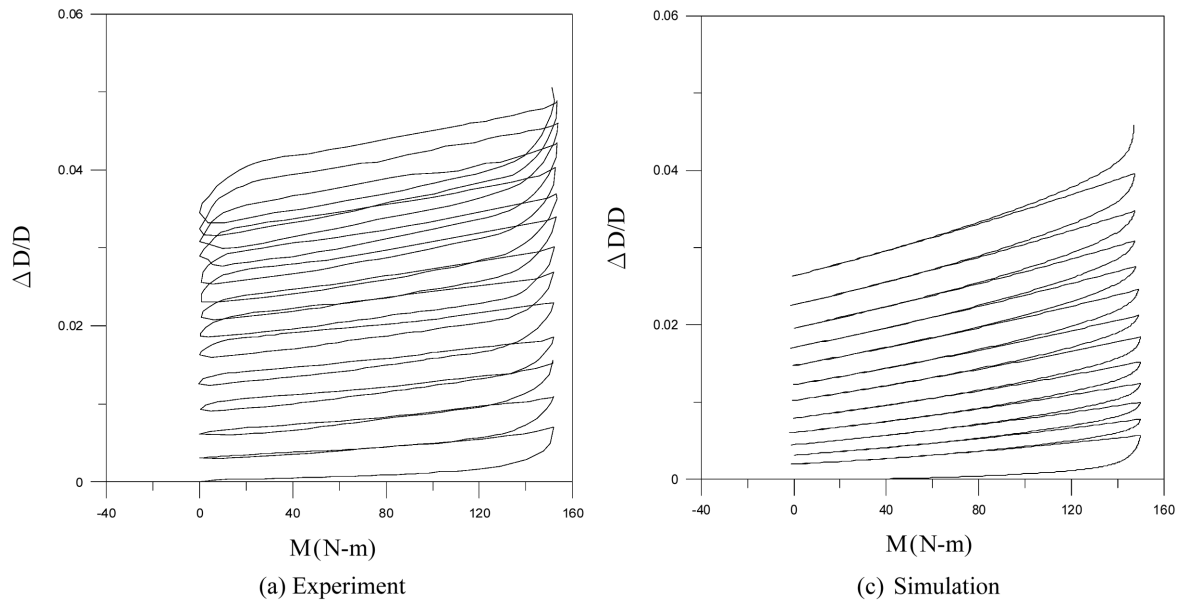


Fig. 12 Experimental and simulated cyclic ovalization ($\Delta D/D$)-moment (M) curve where the moment ranges from from + 150 to 0 N-m ($r = 0$)

speed of the loop with a larger r is faster than that of a loop with a smaller r . Although the ratcheting speed of the loop moving to the right slows down, it does not reach a steady state. Figs. 9(b) and 11(b) depict the corresponding theoretical results for Figs. 9(a) and 11(a), respectively. Figs. 10(a) and 12(a) show the corresponding experimental results of the cyclic $\Delta D/D$ - M curve. It can be seen that the ovalization grows to a maximum value at the controlled maximum moment on first loading. However, ovalization does not increase for continuous reverse bending to the minimum moment. The ovalization increases in an unsymmetrical and ratcheting manner with the number of bending cycles. In addition, the curve has a bias in the direction of the mean moment. Figs. 10(b) and 12(b) depict the corresponding theoretical results for Figs. 10(a) and 12(a), respectively.

4.2 Collapse of SUS 304 stainless steel tubes under moment-controlled symmetric and unsymmetric cyclic bending

Fig. 13 shows the experimental results of the moment range (ΔM) versus the number of cycles necessary to produce buckling (N_b) with three different values of r (-1 , -0.5 and 0), respectively. The magnitudes of ΔM vary from 400 to 150 N-M. For each r , five or six specimens were carefully tested in order to construct the ΔM - N_b curve. It was found that the collapse of circular tubes subjected to cyclic bending is strongly influenced by the magnitude of the mean moment. It can also be seen from Fig. 13 that for a certain amount of ΔM , the specimen with a higher r leads to a lower number of cycles necessary to produce buckling. The same results of Fig. 13 are plotted on a log-log scale and are shown in Fig. 14(a). The three straight dashed lines in this figure, determined by the least square method, denote the three different amounts of r .

In 1987, Kyriakides and Shaw (1987) proposed the relationship between the cyclic curvature κ_c

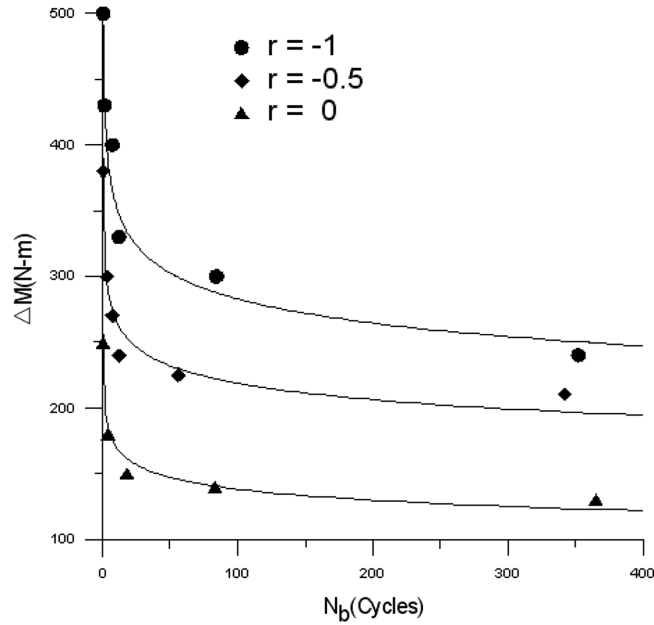


Fig. 13 Experimental results of the moment range (ΔM) versus the number of cycles necessary to produce buckling (N_b) curves for three different values of r

(maximum curvature for symmetric cyclic bending) and the number of cycles necessary to produce buckling N_b to be given by

$$\kappa_c = A(N_b)^{-\alpha} \tag{20}$$

where A and α are material parameters, which are related to the material properties and the D/t ratio. The constant A is the magnitude of cyclic curvature at $N_b = 1$, and is the slope on the log-log plot. Eq. (20) has been widely used for simulating curvature-controlled cyclic bending tests. However, after having considered the results of presented the moment-controlled cyclic bending tests here, it is proposed Eq. (20) be modified to

$$\Delta M = A(N_b)^{-\alpha} \tag{21}$$

or

$$\log \Delta M = \log A - \alpha \log N_b \tag{22}$$

where ΔM is the controlled moment range, and α and A are material constants, which are related to the material properties, the D/t ratio and r . However, only one material (SUS 304 stainless steel) with a constant D/t ratio ($= 60$) was used in the tests presented in this study. Nevertheless, the material constants α and A are considered to be only related to r . Since the three straight dashed lines in Fig. 14(a) are almost parallel, it appears the material constant α has no correlation to the magnitude of r . Thus, following function is proposed to describe the material constant A ,

$$A = a(r + 1) + b \tag{23}$$

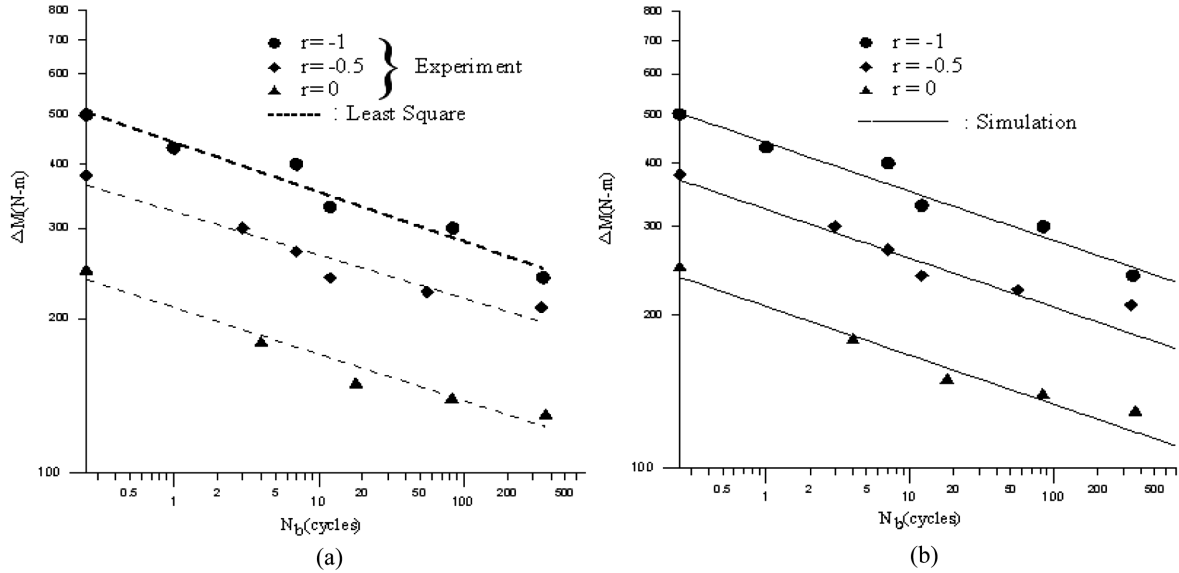


Fig. 14 (a) Experimental results of the moment range (ΔM) versus the number of cycles necessary to produce buckling (N_b) curves for three different values of r on a log-log scale, (b) theoretical simulated results

where a and b are material parameters. When we consider the case of $r = -1$ (symmetric cyclic bending), the magnitude b is equal to A from Eq. (23). By using the experimental data for the case of $r = -1$ in Fig. 14(a), the magnitudes of α and b can be determined from Eq. (22) resulting $\alpha = 0.0969$ and $b = 439.65$ N-m. On the basis of two straight lines where $r = -0.5$ and 0 in Fig. 14(a), the magnitude of a can be determined to be -231.22 N-m. The results correlating to the material parameters are shown in Fig. 14(b). The simulated results are in good agreement with the obtained experimental results.

4.3 Critical ovalization at collapse

Fig. 15 shows the relationship between of the moment range (ΔM) and the critical magnitude of ovalization $(\Delta D/D)_b$ at collapse for three different values of r (-1 , -0.5 and 0). It can be seen that for a certain amount of r , the quantity $(\Delta D/D)_b$ increases when the value of ΔM increases. In addition, for a certain amount of ΔM , the specimen with a higher r leads to a higher amount of $(\Delta D/D)_b$. This phenomenon is in stark contrast to previous investigations of curvature-controlled symmetric cyclic bending tests (Kyriakides and Shaw 1987, Pan and Her 1998, and Lee and Pan 2001) and curvature-controlled unsymmetric cyclic bending tests (Pan and Lee 2002). In the above mentioned investigations, an almost constant amount of $(\Delta D/D)_b$ was obtained for tubes of a certain material subjected to symmetric or unsymmetric curvature-controlled cyclic bending.

The results of Fig. 15 are plotted on a log-log scale and shown in Fig. 16(a). The three straight dashed lines in this figure, determined by the least square method, denote the three different amounts of r . An empirical formula for the relationship between $(\Delta D/D)_b$ and ΔM is proposed as

$$(\Delta D/D)_b = B(\Delta M)^\phi \quad (24)$$

or

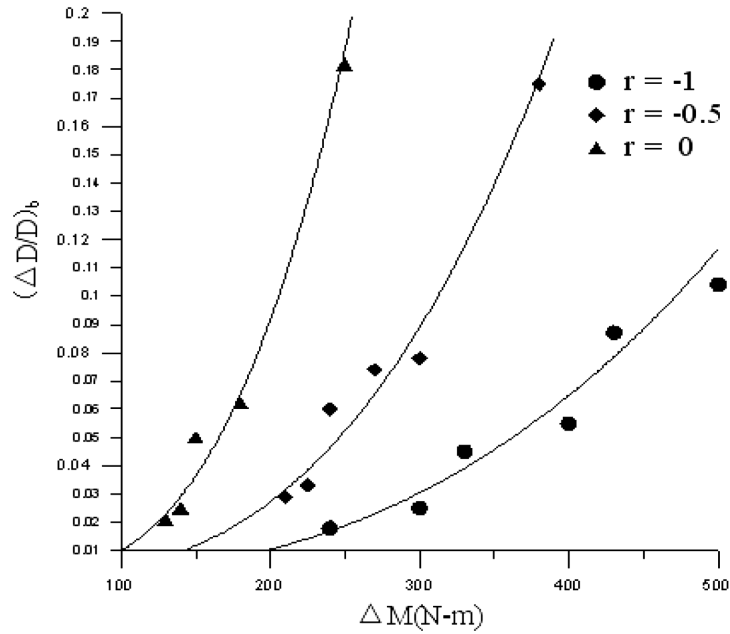


Fig. 15 The experimental results of the critical magnitude of ovalization $(\Delta D/D)_b$ at collapse versus the moment range (ΔM) for $r = -1, -0.5$ and 0

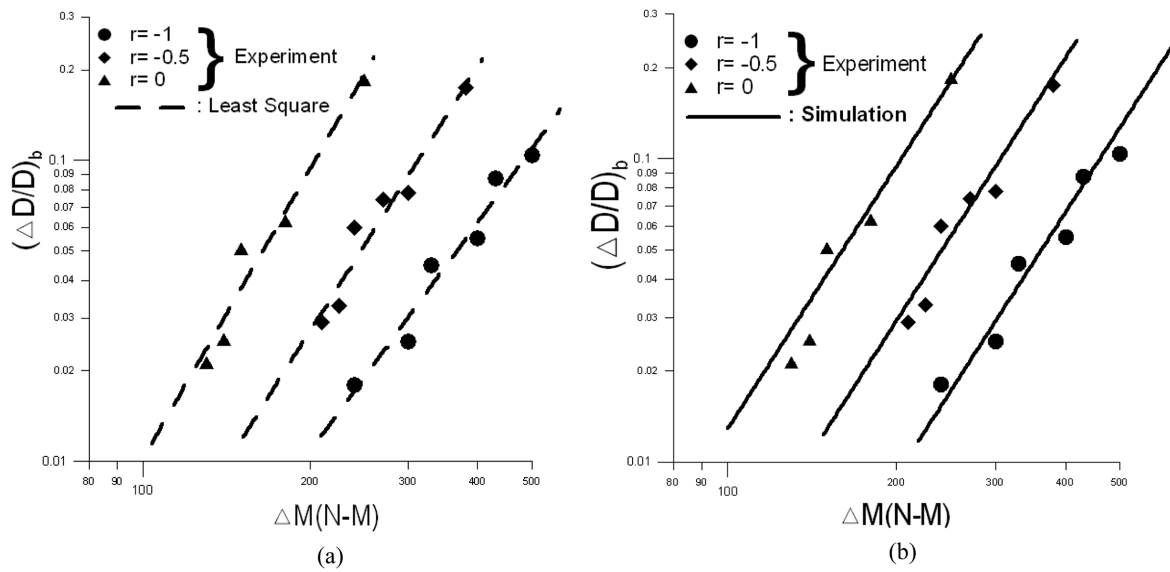


Fig. 16 (a) The experimental results of the moment range (ΔM) versus the critical magnitude of ovalization $(\Delta D/D)_b$ at collapse for three different values of r on a log-log scale, (b) the theoretical simulated result

$$\log (\Delta D/D)_b = \log B + \phi \log \Delta M \tag{25}$$

where B and ϕ are material constants, which are related to the moment ratio r . Although the three

groups of tested specimens had three different stress ratios, three almost parallel straight lines can be seen. Therefore, the slope of these lines φ is a constant, which can be approximated to 2.88, as seen in Fig. 16(a). For the material constant B, the empirical function

$$B = 10^{c(c+1)+d} \quad (26)$$

is proposed, where c and d are material parameters. In this study, the magnitude of d can be determined by using the case of $r = -1$, and is -8.67 . Based on the variation of the two straight lines of $r = -0.5$ and 0 in Fig. 16(a), the magnitude of c can be determined to be 1.02 . The correlating results based on the determined material parameters are shown in Fig. 16(b). Again, the simulation is in good agreement with the experimental results.

5. Conclusions

In this study, the effect of the mean moment on the response and collapse of thin-walled tubes subjected to cyclic bending was investigated. According to the experimental and theoretical results, the following important conclusions are apparent from this investigation:

- (1) For symmetric moment-controlled cyclic bending ($r = -1$), the first M- κ loop is on the left side, but the subsequent M- κ loops gradually move to the right side and become stable after several cycles (Fig. 7(a)). However, the $\Delta D/D$ - M curve shows a symmetric, ratcheting and increase with the number of bending cycles (Fig. 8(a)). For unsymmetric moment-controlled cyclic bending ($r = -0.5$ or 0), the M- κ curve increases with the number of cycles in a ratcheting manner and gradually moves to the right (Figs. 9(a) and 11(a)). However, the $\Delta D/D$ - M curve increases in an unsymmetrical, slant, and ratcheting manner with the number of bending cycles (Figs. 10(a) and 12(a)). Endochronic theory and the principle of virtual work were used to simulate the relationship between the moment, curvature and ovalization of thin-walled tubes under symmetric and unsymmetric cyclic bending. Reasonable correlation between the experimental data and the theoretical simulation was achieved.
- (2) It was determined from the ΔM - N_b plot (Fig. 13) that the collapse of circular tubes subjected to cyclic bending is strongly influenced by the magnitude of the mean moment. A specimen with a higher r (higher mean moment) leads to a lower number of cycles necessary to produce buckling for a same magnitude of ΔM . Based on the trend of the ΔM - N_b plot on a log-log scale (Fig. 14(a)), and empirical formula (Eq. (21)) was proposed to simulate the relationship between ΔM and N_b for different values of r .
- (3) The $(\Delta D/D)_b$ - ΔM plot (Fig. 15) demonstrates that the value of $(\Delta D/D)_b$ is not a constant for moment-controlled symmetric or unsymmetric cyclic bending. For a certain amount of ΔM , the specimen with a higher value of r leads to a higher amount of $(\Delta D/D)_b$. For a certain amount of r , the specimen with a higher controlled ΔM leads to a higher magnitude of $(\Delta D/D)_b$. Similarly, based on the trend of the $(\Delta D/D)_b$ - ΔM plot on a log-log scale (Fig. 16(a)), and empirical formula (Eq. (24)) was proposed to simulate the relationship between $(\Delta D/D)_b$ and ΔM for different values of r .

Acknowledgements

The work presented was carried out with the support of the National Science Council under grant NSC 90-2212-E-006-070. Its support is gratefully acknowledged.

References

- Corona, E. and Kyriakides, S. (1988), "On the collapse of inelastic tubes under combined bending and pressure", *Int. J. Solids Struct.*, **24**(5), 505-535.
- Corona, E. and Kyriakides, S. (1991), "An experimental investigation of the degradation and buckling of circular tubes under cyclic bending and external pressure", *Thin Wall. Struct.*, **12**, 229-263.
- Corona, E. and Vaze, S. (1996), "Buckling of elastic-plastic square tubes under bending", *Int. J. Mech. Sci.*, **38**(7), 753-775.
- Elchalakani, M., Zhao, X.L. and Grzebieta, R.H. (2002), "Plastic mechanism analysis of circular tubes under pure bending", *Int. J. Mech. Sci.*, **44**, 1117-1143.
- Elchalakani, M., Zhao, X.L. and Grzebieta, R.H. (2004), "Concrete-filled circular tubes subjected to constant amplitude cyclic pure bending", *Eng. Struct.*, **26**, 2125-2135.
- Fabian, O. (1977), "Collapse of cylindrical, elastic tubes under combined bending, pressure and axial loads", *Int. J. Solids Struct.*, **13**, 1257-1273.
- Fan, J. (1983), "A comprehensive numerical study and experimental verification of endochronic plasticity", *Ph.D. Dissertation*, Department of Aerospace Engineering and Applied Mechanics, University of Cincinnati.
- Gellin, S. (1980), "The plastic buckling of long cylindrical shells under pure bending", *Int. J. Solids Struct.*, **16**, 397-407.
- Jiao, H. and Zhao, X.L. (2004), "Section slenderness limits of very high strength circular steel tubes in bending", *Thin Wall. Struct.*, **42**, 1257-1271.
- Kyriakides, S. and Shaw, P.K. (1982), "Response and stability of elastoplastic circular pipes under combined bending and external pressure", *Int. J. Solids Struct.*, **18**(11), 957-973.
- Kyriakides, S. and Shaw, P.K. (1987), "Inelastic buckling of tubes under cyclic loads", *J. Press. Vessel Technol.*, ASME, **109**, 169-178.
- Lee, K.L. and Pan, W.F. (2001), "Viscoplastic collapse of titanium alloy tubes under cyclic bending", *Struct. Eng. Mech.*, **11**(3), 315-324.
- Lee, K.L., Pan, W.F. and Hsu, C.M. (2004), "Experimental and theoretical evaluations of the effect between diameter-to-thickness ratio and curvature-rate on the stability of circular tubes under cyclic bending", *JSME Int. J., Series A*, **47**(2), 212-222.
- Lee, K.L., Pan, W.F. and Kuo, J.N. (2001), "The influence of the diameter-to-thickness ratio on the stability of circular tubes under cyclic bending", *Int. J. Solids Struct.*, **38**, 2401-2413.
- Pan, W.F. and Chern, C.H. (1997), "Endochronic description for viscoplastic behavior of materials under multiaxial loading", *Int. J. Solids Struct.*, **34**(17), 2131-2159.
- Pan, W.F. and Fan, C.H. (1998), "An experimental study on the effect of curvature-rate at preloading stage on subsequent creep or relaxation of thin-walled tubes under pure bending", *JSME Int. J., Series A*, **41**(4), 525-531.
- Pan, W.F. and Her, Y.S. (1998), "Viscoplastic collapse of thin-walled tubes under cyclic bending", *J. Eng. Mater. Tech.*, ASME, **120**, 287-290.
- Pan, W.F. and Lee, K.L. (2002), "The effect of mean curvature on the response and collapse of thin-walled tubes under cyclic bending", *JSME Int. J., Series A*, **45**(2), 309-318.
- Pan, W.F., Lee, T.H. and Yeh, W.C. (1996), "Endochronic analysis for finite elasto-plastic deformation and application to metal tube under torsion and metal rectangular block under biaxial compression", *Int. J. Plast.*, **12**(10), 1287-1316.
- Pan, W.F., Wang, T.R. and Hsu, C.M. (1998), "A curvature-ovalization measurement apparatus for circular tubes under cyclic bending", *Exp. Mech.*, **38**(2), 99-102.

- Reddy, B.D. (1979), "An experimental study of the plastic buckling of circular cylinders in pure bending", *Int. J. Solids Struct.*, **15**, 669-682.
- Shaw, P.K. and Kyriakides, S. (1985), "Inelastic analysis of thin-walled tubes under cyclic bending", *Int. J. Solids Struct.*, **21**(11), 1073-1110.
- Valanis, K.C. (1980), "Fundamental consequence of a new intrinsic time measure-plasticity as a limit of the endochronic theory", *Arch. Mech.*, **32**, 171-191.
- Vaze, S. and Corona, E. (1998), "Degradation and collapse of square tubes under cyclic bending", *Thin Wall. Struct.*, **31**, 325-341.